Photocatalytic Degradation of reactive violet 1 by Polyorthotoluidine/Titanium dioxide nanocomposite

Muhammad Naveed Anjum[1*], Sufyan Qasim[1], Mirza Nadeem Ahmad[1], Sarosh Iqbal[1], Shazia Abrar[1], Zubair Nabi[1]

1. Department of Applied Chemistry, Government College University Faisalabad 38000, Pakistan.

Corresponding author: anjumccj@hotmail.com

GRAPHICAL ABSTRACT

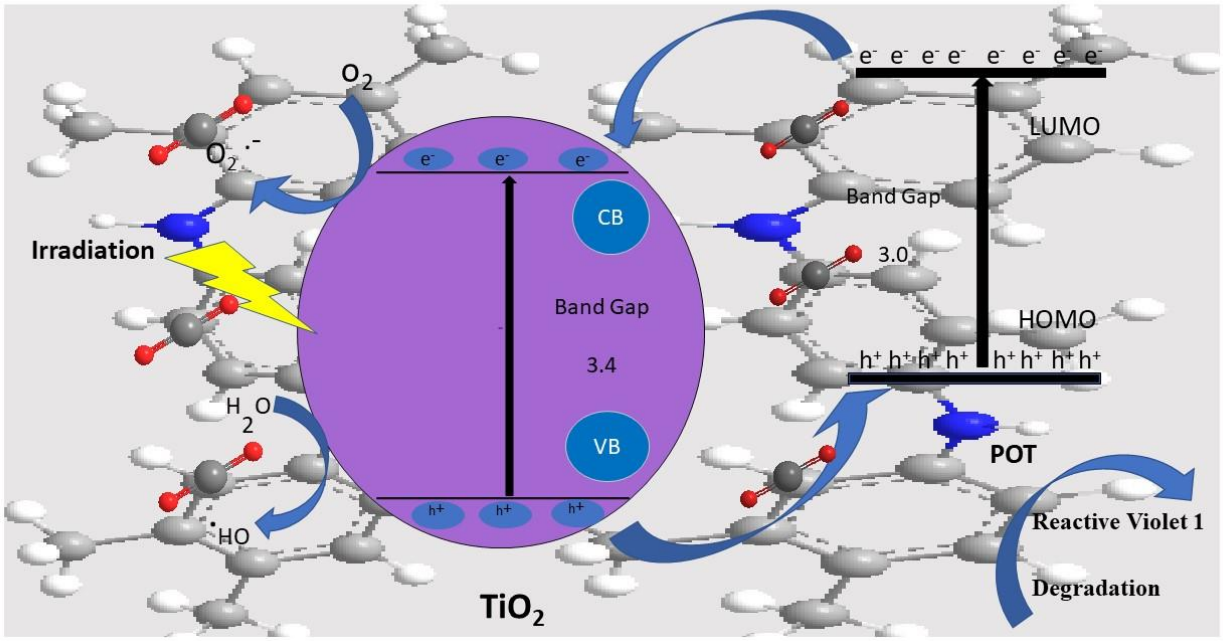

ABSTRACT

Conducting poly(o-toluidine) (POT)/titanium dioxide (TiO_2) nanocomposite have been synthesized by in situ chemical oxidation polymerization of o-toluidine in the presence of TiO_2 nanoparticles. The various composites were synthesized by changing the percentage load of titanium dioxide nanoparticles in poly-ortho-toluidine matrix. The synthesized nanocomposites were characterized by using Scanning electron microscopy (SEM), X-Rays diffraction (XRD), and Fourier transform infrared spectroscopy (FTIR). The POT/TiO_2 nanocomposites were further employed to evaluate the photocatalytic potential of the composite materials towards reactive violet 1.

Keywords: Photocatalytic Degradation, Nanocomposites, Reactive Violet 1, Water Pollution, Dye Degradation.

1. Introduction

Among the natural resources water is most important necessity and is considered to be fundamental for existence of all living beings including human, economic development, and production of food. Now we require water conservation to save the globe and secure the future of humans. With the development of our lifestyle and civilization that is accomplishing new heights, now living organisms are paying a very big price for this development (Apostol et al., 2012). Due to advancements in all fields such as in agriculture, industry, and new growing technologies are using more and more chemicals. Chemicals used in these industries have a great impact on the environment and contaminate the water (Al-Bastaki, 2004). Organic and inorganic chemicals used in industrial activities produce a large volume of contaminated water which causes hazardous health problems in humans and other living organisms (Behnajady et al., 2006). There are many sources of chemicals such as dyes used in the paper industry, printing industry, food, and plastic industry. These industries are the main sources of colored substances in wastewater (Erfani and Javanbakht, 2018).

Many physical, biological, and chemical techniques have been used for the removal and degradation of dyes from wastewater (Liu et al., 2007; Ahmad et al., 2022). These techniques include separation by using membrane, chemical oxidation, adsorption, degradation using microbes, electrochemical method, photocatalytic method, and coagulation. These all techniques have very good outcomes and are widely used all over the world for dye removal (Rafiee et al., 2020; Mobin and Tanveer, 2012; Ahmad et al., 2020).

In the advanced oxidation process, photocatalysis is an emerging and efficient method for the treatment of several dyestuffs. In this process, TiO_2, and CdS have the most commonly studied photocatalysts (Campos et al., 2019). But among the various materials used for photocatalysis,

TiO_2 is the finest photocatalyst, which is extensively utilized for the photcatalytic degradation of dye (Ullah and Dutta, 2008; Tang, Z et al., 2021; Nadeem et al., 2018).

For the surface modification of TiO_2, different physical and chemical methods have been utilized for TiO_2 particles (Jamil and Fasehullah 2021). The most important and efficient method for surface modification is the wrapping of TiO_2 particles as core by the polymeric shell using conducting polymers under visible light irradiation, their photocatalytic performance has been investigated against different chemicals (Khan et al., 2020; Neppolian et al., 2002; Rafiee et al., 2020; Zan et al., 2004; Anjum et al., 2014). The conducting polymers enhance the photocatalytic potential of TiO_2 by circulating the free electrons (Shehzad et al., 2016; Shehzad et al., 2014). Polyorthotoluidine is one of the extensively used conducting polymers because of its cheap production cost, stability, ease to prepare, and reversible acid-base chemistry, (Konstantinou and Albanis, 2004; Olad and Nosrati, 2012; Hussain et al., 2018; Ahmad et al., 2018). In the current study, the POT/TiO_2 nanocomposites was tested for the photocatalytic degradation of dye (reactive violet 1) in aqua media under ultraviolet irradiation.

2. Materials and Methods

2.1. Chemicals

o-toluidine monomer, potassium persulphate (KPS), hydrochloric acid, and titanium dioxide (~ 50nm) were procured from Sigma Aldrich used as received and Methanol acetic acid.

2.2. Synthesis of TiO_2 NPs

The acetic acid hydrolysis approach was used to prepare TiO_2 nanoparticles. The solution of acetic acid (1M) was prepared by using distilled H_2O under continuous stirring for 30 minutes then, 0.5M solution of titanium isopropoxide was poured into the acidic solution and stirred at 50 °C for 6 hours. A greyish-colored material was formed. That was separated by centrifuge and dried a room temperature (Zhou et al 2016).

Regeneration of TiO_2

TiO_2 nanoparticles were regenerated by adding 10g TiO_2 in 20 ml of 0.1M HNO_3 solution under continuous stirring by a magnetic stirrer for 24 hours. Then it was sonicated for 2 hours to prevent agglomeration. Finally, it was separated and dried at 70 °C in an electric oven.

2.3. Synthesis of POT/TiO_2 nanocomposites

POT/TiO_2 nanocomposites were synthesized in three different compositions which are mentioned in (Table 1).

Table 1 Compositions of POT/TiO_2

Sample name	POT	TiO_2	Ratio
Composition 1 (S1)	2ml	10g	1:5
Composition 2 (S2)	2ml	5g	2:5
Composition 3 (S3)	2ml	20g	1:10

First of all, 1 molar solution of HCl was prepared by diluting the concentrated HCl by using the dilution formula. Three different samples (S1, S2, & S3) were prepared by loading the TiO_2 NPs (10g, 5g, & 20g) in the POT matrix, respectively (Anwar et al., 2015). Then, 100 ml of 1M HCl was taken in a beaker and TiO_2 powder was dispersed in it by magnetic stirring for 30 minutes. After that, 2 ml of ortho-toluidine was added to the acidic solution. Then, another solution comprising 25 ml of distilled water and 5g of potassium persulphate (KPS) was prepared. The KPS solution was added into the monomer solution and the reaction mixture was allowed to polymerize under constant stirring for 3 hours at room temperature. After 3 hours of constant stirring, a blackish green colored gel was obtained. The sample was then separated by centrifugation at 4000 rpm for 5 minutes. The sample was washed several times with water then

with ethanol for complete removal of solvent and impurities. The sample was dried in an electric oven at 80 °C for 2 hours. Similarly, other samples were prepared by varying the amount of TiO_2 NPs. After that obtained solid is converted into a fine powder which is POT/TiO_2 nanocomposite. The samples have further proceeded for characterization.

3. Results and discussion

3.1. Fourier-transform Infrared Spectroscopy (FTIR)

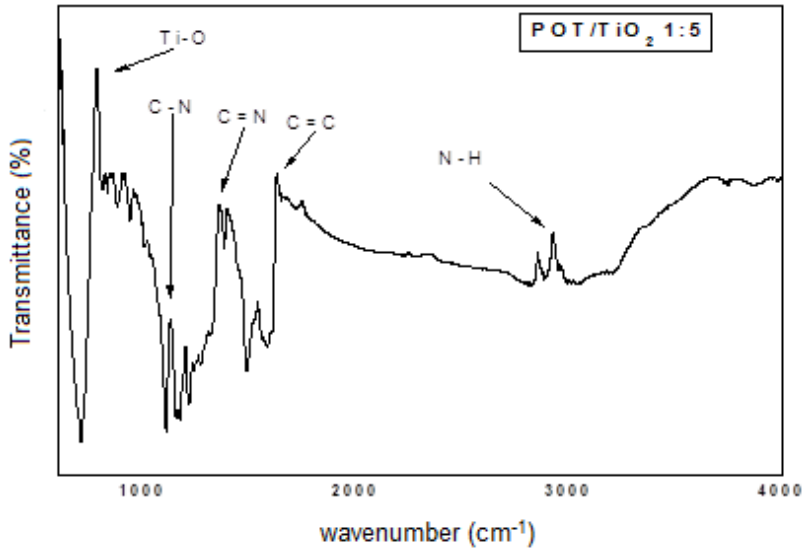

Fig. 1 FT-IR spectrum of POT/TiO_2 sample (S1)

The FT–IR spectrum of sample S1 of POT/TiO_2 nanocomposite was presented in (Fig. 1). The FT–IR spectrum showed a vibrational peak at 711 cm^{-1} due to the presence of Ti–O bond (Zhou et al., 2016). The wide peak at 3032 cm^{-1} and 2882 cm^{-1} was associated with N–H stretching vibration. The peaks at 1487 cm^{-1} and 1585 cm^{-1} exhibited C=N and C=C stretching vibrations for the benzenoid and quinoid structures. While the signal at 1382 cm^{-1} indicated that the benzenoid units were in the C–N stretching phase. The signal in the spectrum at 882 cm^{-1} was allocated to the out of plane C–H vibrational mode which confirmed the formation of POT/TiO_2 (Zan et al., 2004).

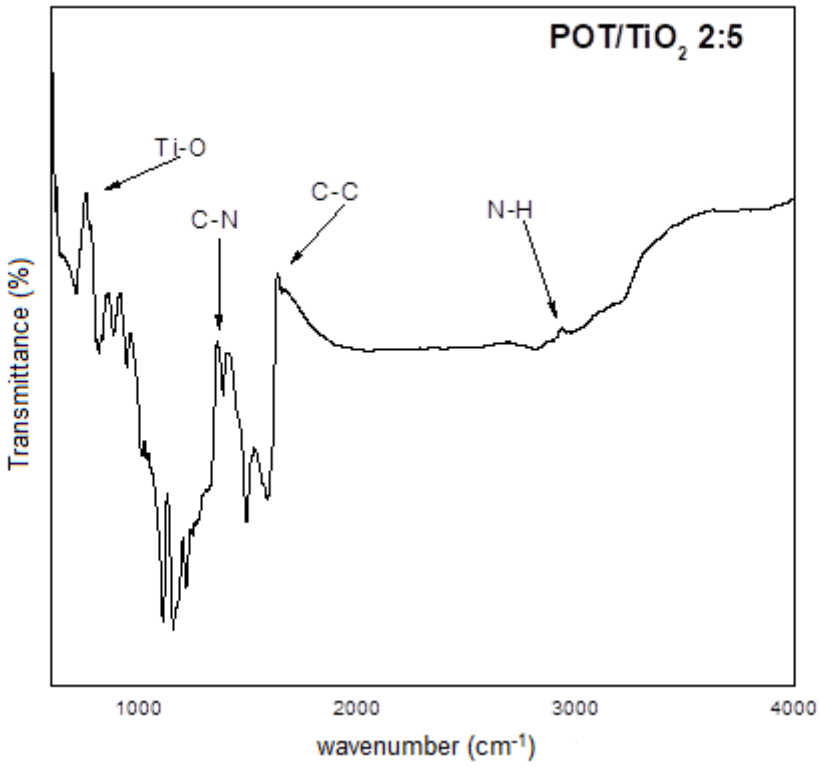

Fig. 2 FT-IR spectrum of POT/TiO_2 sample (S2)

The FTIR spectrum of POT/TiO_2 nanocomposite was shown in (Fig. 2). Due to the Ti–O vibrations, the FT–IR spectrum displayed a peak at 710 cm^{-1}. The peaks observed in the spectrum, at 1488 cm^{-1} and 1586 cm^{-1}, showed the C–C stretching vibration of the benzenoid and quinoid structure respectively. Moreover, aromatic amine contain C-N stretching was showed peak at 1382 cm^{-1}. The out of plane and in-plane C–H bending modes were given to the peaks that emerged at 812 cm-1 and 1154 cm-1, respectively. The peak detected at 1213 cm^{-1} indicated the N–H bond of an amine of the aromatic ring (Konstantinou and Albanis, 2004; Pham et al., 2022).

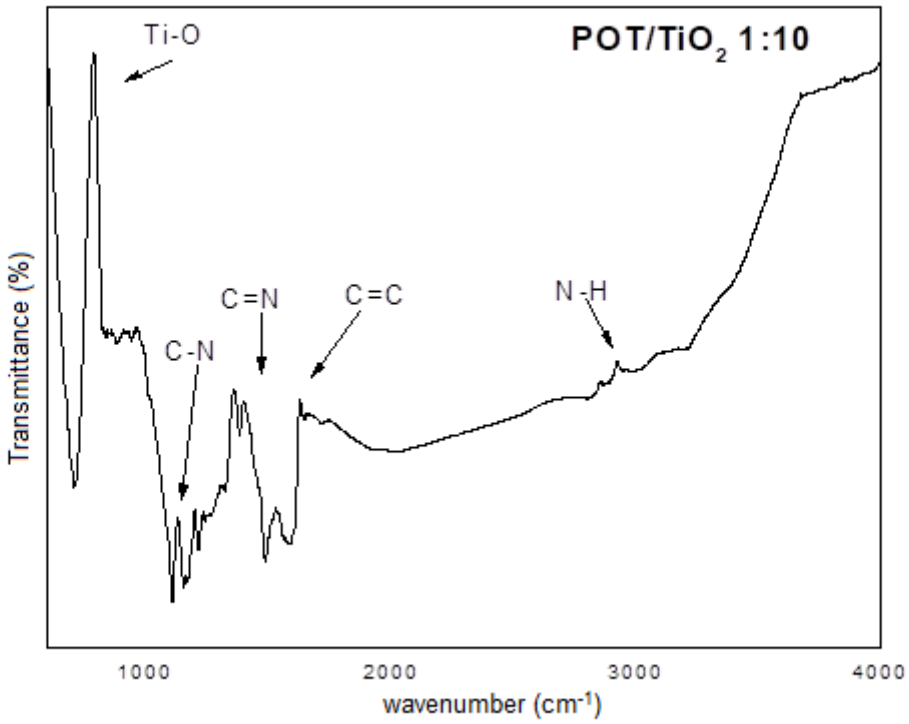

Fig. 3 FT-IR spectrum of POT/TiO_2 sample (S3)

The FT–IR spectrum of sample S3 of POT/TiO_2 nanocomposite was given in (Fig. 3). The FT–IR spectrum showed a broad peak at 706 cm^{-1} due to Ti–O vibrations. And all other peaks were the same as for samples S1 and S2. This proved the formation of POT/TiO_2 nanoparticles.

In spectra of POT/TiO_2 nanocomposites, most of the peaks for POT were observed as reported (Gayathri and Balan 2019; Shehzad et al., 2013) except a peak at 1161.70 cm^{-1}, this peak was slightly changed its position and shifted to 1174 cm^{-1} for the spectra of POT/TiO_2 nanocomposites. This shifting of peak confirmed that delocalization was greater due to the full contact between the TiO_2 nanoparticles and the POT matrix. Consequently, it is concluded that the shifting of peaks to some extent was due to the interaction of POT and TiO_2 nanoparticles in composite materials (Shakir et al., 2014).

3.2. Scanning Electron Microscopy (SEM)

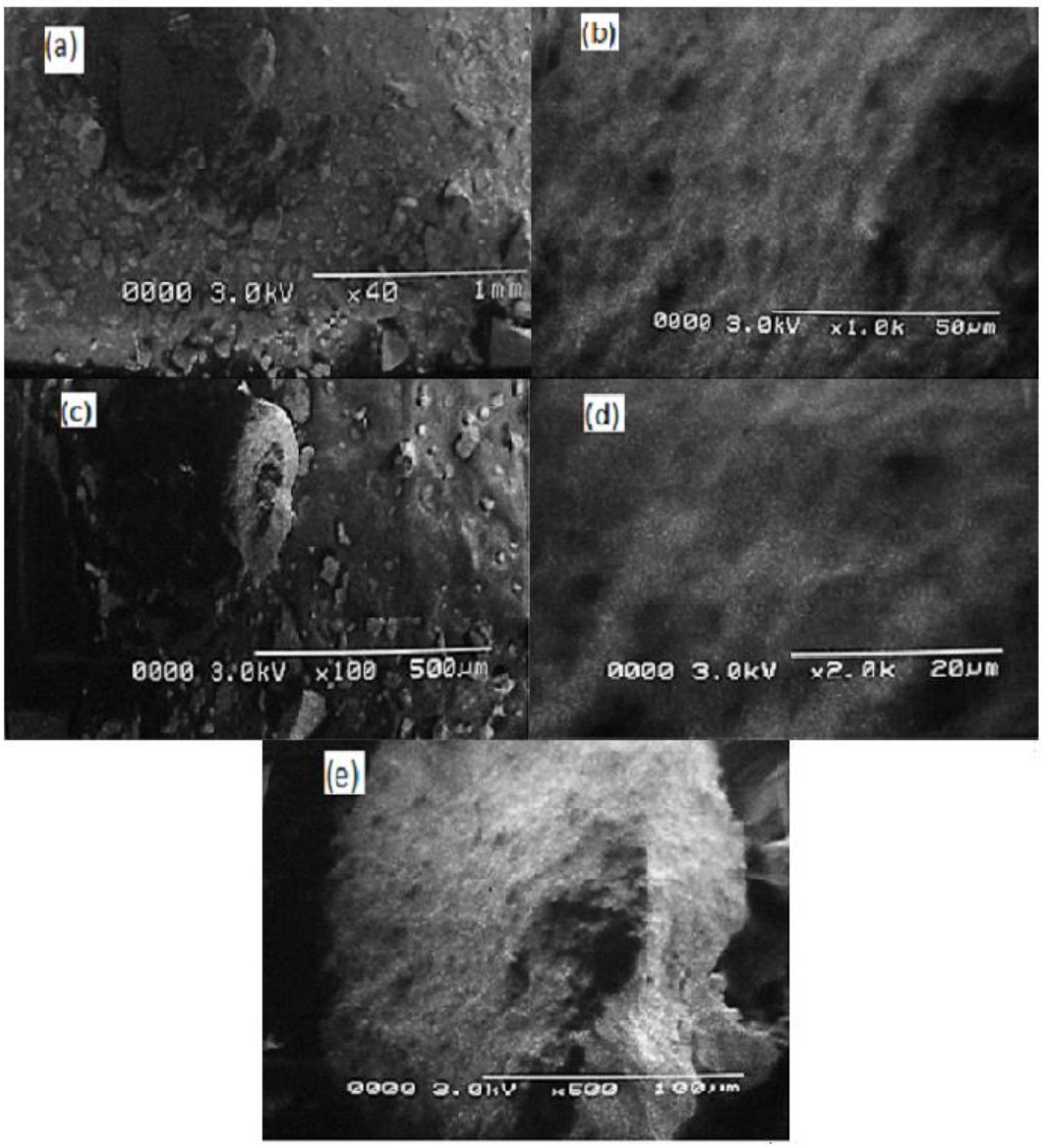

Fig. 4 SEM images of POT/TiO_2 nanocomposite Sample (S1)

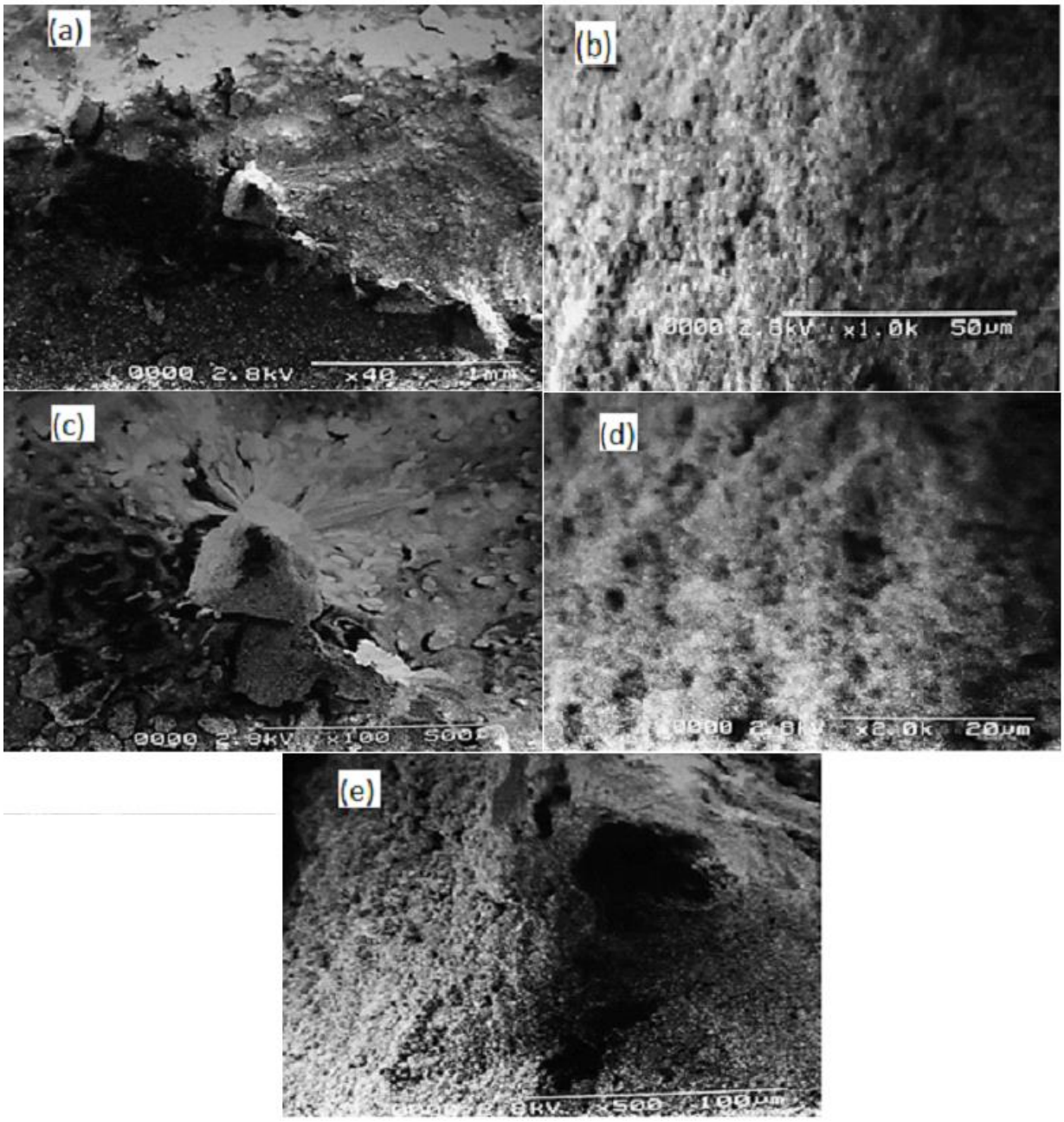

Fig. 5 SEM images of POT/TiO_2 nanocomposite Sample (S2)

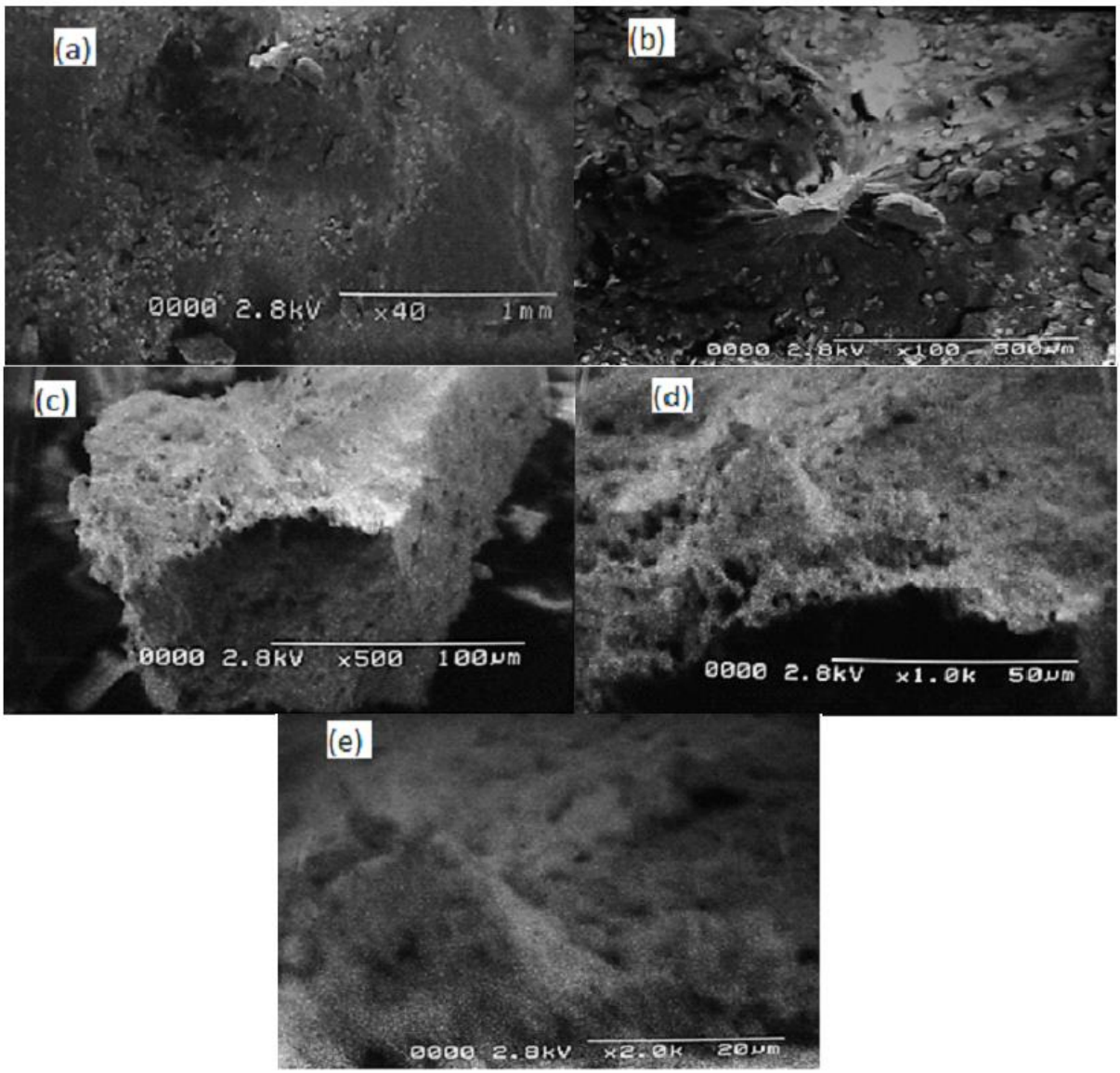

Fig. 6 SEM images of POT/TiO_2 nanocomposite Sample (S3)

The SEM images of all 3 samples (S1, S2, S3) labeled on (Fig. 4, 5, and 6) showed the structure characteristics and morphologies of POT/TiO_2 nanocomposite. The white spots showed the presence of TiO_2 in all 3 figures. In Fig. 4, the spreading of TiO_2 nanoparticles was observed throughout the POT matrix. These images showed the core-shell structure of the nanocomposite. Irregular clusters were shown in these images which indicated the uniform diffusion of titanium dioxide nanoparticles in the matrix of polyorthotoluidine. These figures also showed the porous morphology which explained the adsorption properties of the polymer. It also exhibited a granular

structure (Matei et al., 2008). In Fig. 4 (d), there was a large granule collection on the POT/TiO_2 nanocomposite (Zan et al., 2004; Hussain et al., 2017). In other images of SEM 5 and 6 similar features were observed for S2 and S3 in the respective figures.

3.3. X-ray diffraction analysis

XRD technique is used to determine the structure of different nanocomposites. POT/TiO_2 nanocomposite structures have been examined by using X-ray diffraction. To identify the sample's phase and crystallinity, XRD measurements were recorded. Figure 7 showed the XRD outlines of the POT/TiO_2 composite. The XRD pattern of the POT/TiO_2 NC for sample S1 showed the different peaks whose values of $2\theta°$ were given as: 26.2, 37.1, 39.2, 42.4, 44.1, 55.3, 56.7, 66.8, 67.1, 69.0, and 69.8. That resembled the diffractions of (110), (101), (200), (111), (210), (211), (220), (002), (310), (221) and (301) facets of the TiO_2 rutile phase. It was observed that the results of the prepared nanocomposite were in accordance with the findings given by (Liu et al., 2007). In Fig. 7(a), two wide peaks for POT were observed at the value of $2\theta°$= 5–40 and it was maximum at around 27. Most of the peaks in the spectra became weaker but were in good agreement with them as compared with their pure counterparts. The decreasing intensity in the XRD pattern of sample S1 at 25 could be the inclusion of inorganic particles (Liu et al., 2004).

The X-ray patterns of POT/TiO_2 nanocomposites of sample S2 were shown in Fig. 7(b). The study on X-ray patterns showed different characteristic peaks which were observed in spectra at $2\theta°$= 28, 34, 44, 55, 58, and 64, etc. In spectra, the peak at $2\theta°$ = 25 is for POT that is expected to appear in POT/TiO2 nanocomposite. The TiO_2 nanoparticle size also influenced the crystallite size of the whole nanocomposite. The order of POT < POT/TiO_2 could be owing to the polymerization of *o*-toluidine monomers on TiO_2 surface, encasing TiO_2 nanoparticles. (Shakir et al., 2014).

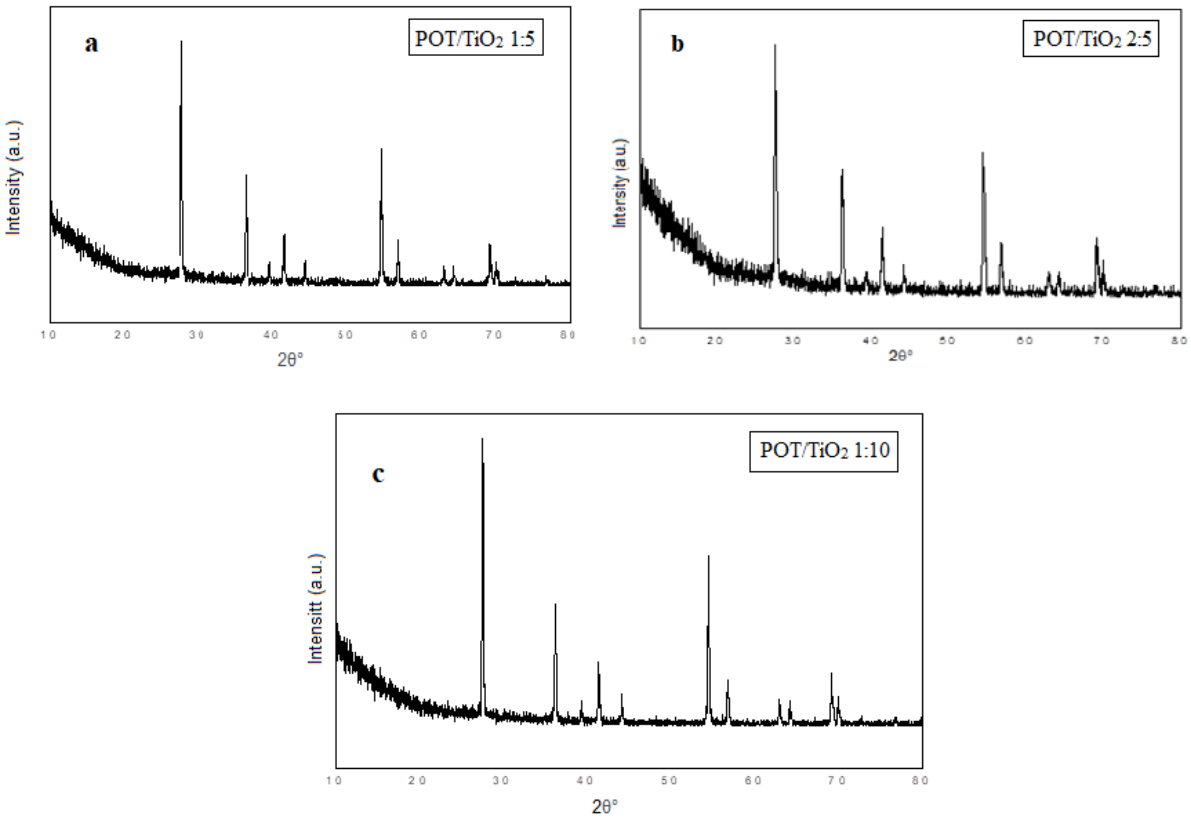

Figure. 7 XRD pattern of POT/TiO_2 sample (S1)

XRD pattern showed four different peaks in the region of 2θ°= 16-26º in fig. 7(c), where the largest peak was round 2θ°= 18.1º. It was imputed that the polymer chains of polyamine were perpendicular, parallel, and repeated after several distances. The second peak present at 2θ°= 20º was also characteristic. It indicated the close contact between the chains. Additionally, the peak present at 2θ°= 24º indicated that the polyorthotoluidine had a very small degree of crystallinity and polyorthotoluidine chains were scattered in the spaces present between the planes. The XRD pattern of the polyorthotoluidine/titanium dioxide nanocomposite indicated that there were very small peaks of titanium dioxide nanoparticles at 2θ°= 32- 38º. These peaks indicated that the molar ratio was very small as compared to polyaniline. The peak at 2θ°= 32.5º explained the crystallinity and wurtzite hexagonal structure of titanium dioxide (Huang et al., 2007; Shehzad et al., 2016).

4. Photocatalytic Activity

To investigate the catalytic efficiency of prepared POT/TiO_2 nanocomposites, a local device was used which had two components. The first was a degradation box and the second was a Xe arc-lamp of 500W. By using this device, the nanocomposites photocatalytic performance was assessed. To study the degradation activity, 100 ml solutions (5mg/L) of dye were prepared in a glass test tube. Then 0.1g of the sample catalyst was added to the dye solution. Keeping the light source off, dye solution was placed in the degradation box. To achieve the equilibrium, the sample dye solution (reactive violet 1) was kept in the degradation box for 1 h under dark and then the dye sample was taken out from the degradation box. The discoloration of dye samples was analyzed using a UV-vis spectrophotometer. Then sample dye solution was placed in a degradation box in the presence of ultraviolet irradiation and the same experiment was carried out. The distance between the sample of dye solution and the light source was kept at 16 cm. The discoloration dye sample was analyzed at different time intervals and by using a spectrophotometer (Abdel-Mottaleb et al., 2019; Anwar et al., 2017; Hussain et al., 2019).

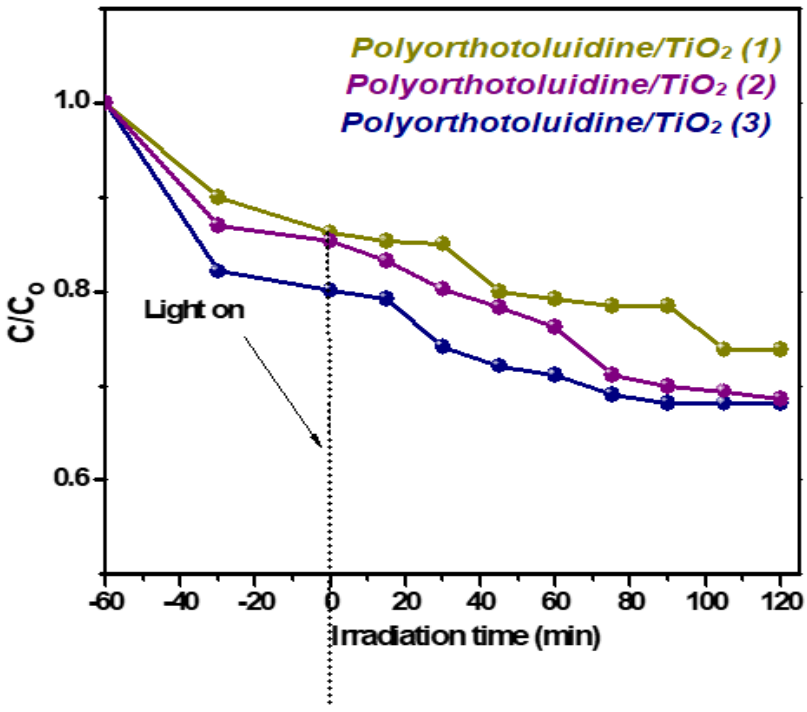

Figure. 10 Photocatalytic degradation curve

The degradation of reactive violet 1 under visible and ultraviolet light was examined by the prepared nanocomposite (S1). This degradation of dye was checked after a different interval of time under visible and ultraviolet light as shown in (Fig. 11). Intensities of dye absorption band were decreased which showed that dye was degraded continuously. It was observed that after 110 minutes there was 26 percent of dye was degraded by the nanocomposite (S1) and after that degradation process was slowed down as shown in (Fig. 11).

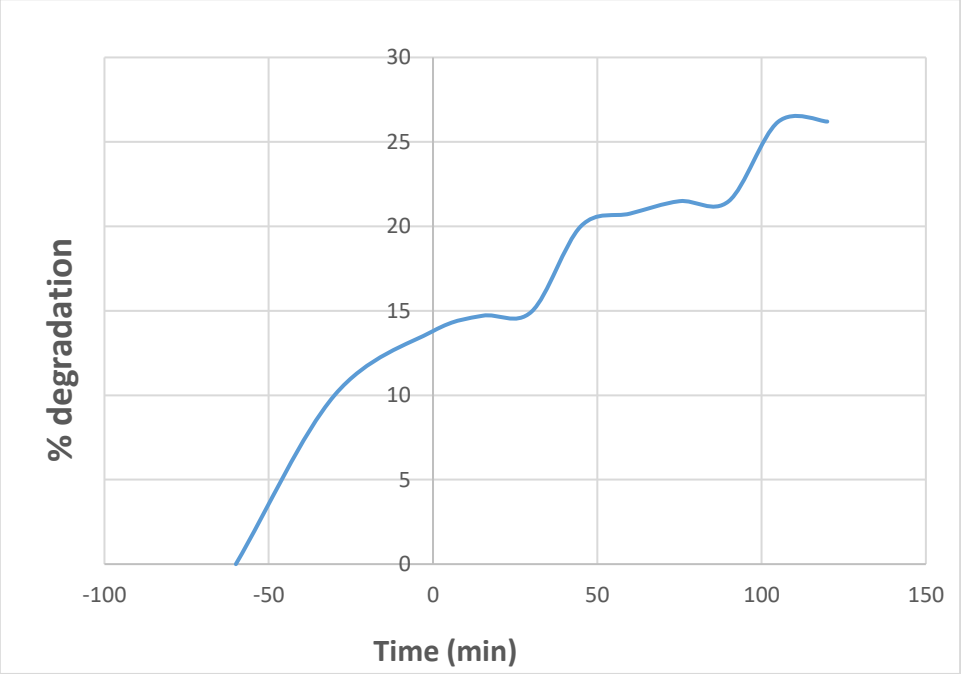

Figure. 11 Percentage degradation efficiency of POT/TiO_2 (S1)

The degradation of reactive violet 1 under visible and ultraviolet light was examined by another prepared nanocomposite (S2). This degradation of dye was checked after a different interval of time under visible and ultraviolet light as shown in (Fig. 12). Intensities of dye absorption band were decreased which shows that dye was degraded continuously. It was observed that after 110 min there was 31 percent of dye was degraded by the nanocomposite (S2) after that degradation process was slowed down as shown in (Fig. 12).

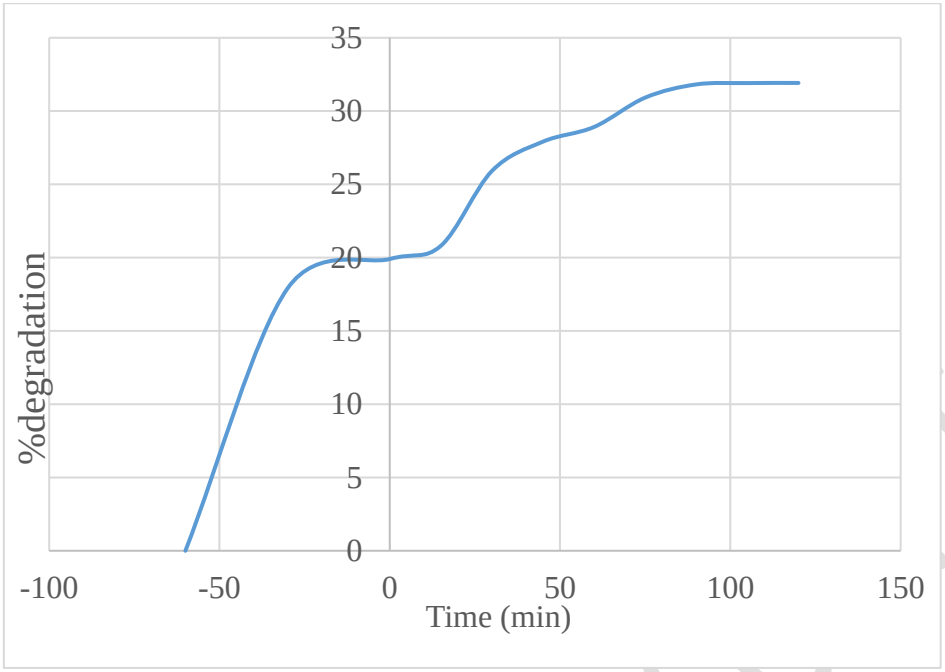

Figure. 12 Percentage degradation efficiency of POT/TiO_2 (S2)

The degradation of reactive violet 1 under visible and ultraviolet light was examined by another prepared nanocomposite (S3). This degradation of dye was checked after different intervals of time under visible and ultraviolet light as shown in (Fig. 13). Intensities of dye absorption band were decreased which showed that dye was degraded continuously. It was observed that after 110 minutes 32 percent of dye was degraded by the nanocomposite (S3) and after that degradation process was slowed down as shown in (Fig. 13).

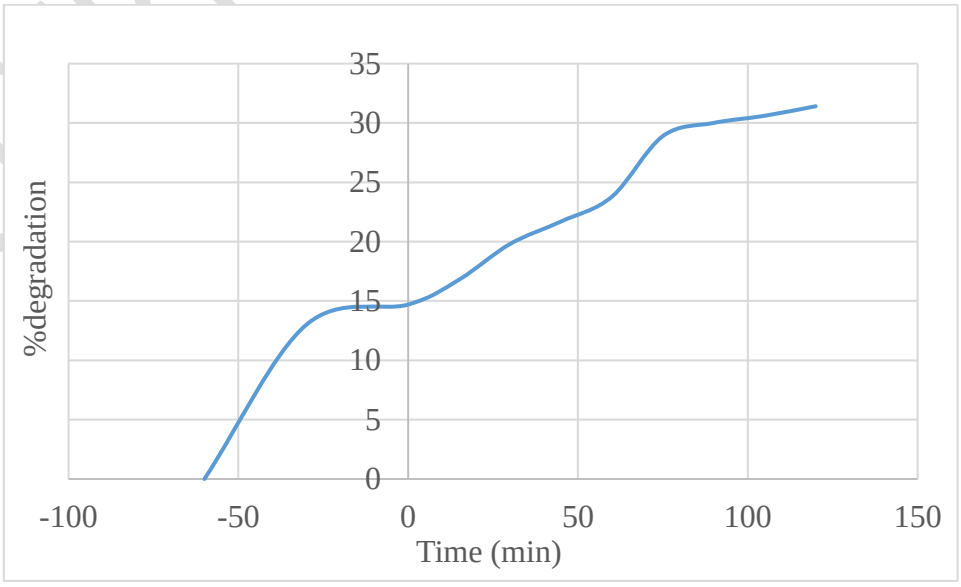

Figure. 13 Percentage degradation efficiency of POT/TiO_2 (S3)

5. Conclusion

In summary, POT/TiO_2 nanocomposites were prepared successfully by using chemical oxidative polymerization techniques. The different analytical approaches were used to confirm the structure and morphology of the produced nanocomposites. The degradation of reactive violet 1 was evaluated under ultraviolet irradiation. The reactive violet 1 degradation was directly related to the amount of TiO_2 in the composite material. The results showed a better potential to degrade reactive violet 1 and other reactive dyes for environmental application.

List of Figures

Sr. No	Figure Name
1	FTIR spectra of POT/TiO_2 sample (S1)
2	FTIR spectra of POT/TiO_2 sample (S2)
3	FTIR spectra of POT/TiO_2 sample (S3)
4	SEM images of POT/TiO_2 nanocomposite Sample (S1)
5	SEM images of POT/TiO_2 nanocomposite Sample (S2)
6	SEM images of POT/TiO_2 nanocomposite Sample (S3)
7	XRD spectra of POT/TiO_2 sample (S1, S2, S3)
8	Photocatalytic degradation curve
9	Percentage degradation efficiency of POT/TiO_2 (S1)
10	Percentage degradation efficiency of POT/TiO_2 (S2)
11	Percentage degradation efficiency of POT/TiO_2 (S3)

List of Tables

Sr. No	Name of tables
1	Compositions of POT/TiO_2 Nanocomposites